Scientia Iranica B (2022) 29(1), 90–100

Sharif University of Technology
Scientia Iranica
Transactions B: Mechanical Engineering
http://scientiairanica.sharif.edu

Effects of chemical reactions, radiation, and activation energy on MHD buoyancy induced nanofluid flow past a vertical surface

G. Lakshmi Devi[a], H. Niranjan[a,*], and S. Sivasankaran[b]

a. *Department of Mathematics, School of Advanced Sciences, Vellore Institute of Technology, Vellore-632014, India.*
b. *Department of Mathematics, King Abdulaziz University, Jeddah 21589, Saudi Arabia.*

Received 28 October 2020; received in revised form 4 February 2021; accepted 19 April 2021

KEYWORDS
Chemical reaction;
Activation energy;
MHD;
Buoyancy force;
Nanofluid;
Thermal radiation.

Abstract. This paper explores the effects of thermal radiation, buoyancy force, chemical reaction, and activation energy on magnetohydrodynamic (MHD) nanofluid flow past a stretching vertical surface. The non-linear momentum, energy, solute, and nanoparticle concentration boundary layer equations are simplified using similarity transformations. The transformed equations are numerically solved using the shooting technique. Corresponding results for dimensionless velocity, temperature, solute, nanoparticle concentration profiles, skin friction, local Nusselt number, local Sherwood number, and local nanoparticle Sherwood number are shown for various related parameters. It is observed that the temperature and concentration profiles of nanoparticles increased with the increase in the parameters of thermal radiation and the temperature difference. With increasing regular buoyancy parameters, the local Nusselt number decreased by increasing the adaptation rate, the Biot number, and the thermal radiation parameters.

1. Introduction

The effect of chemical reactions on Magnetohydrodynamics (MHD) buoyancy-induced nanofluid flow is an important application in many industrial processes, such as chemical coating of flat plates, polymer ejection, and hot rolling as observed by Ibrahim and Makinde [1]. The influence of chemical reaction and activation energy in a mixed convection fluid flow over a stretching sheet studied by Jabeen et al. [2]. Niranjan et al. [3] investigated the chemical reaction effect in MHD mixed convection flow over a plate in a porous medium. They found that in the generative scenario, raising the velocity and concentration profiles increases the chemical reaction parameter, whereas, in the destructive situation, it decreases. Mallikarjuna et al. [4] analyzed the impact of chemical reactions on heat transfer and flow of a viscous nanofluid in a variable porous medium along a vertical cone. Hayat et al. [5] investigated the chemical reaction and double stratification of Williamson nano liquid using a stretched sheet in the MHD stagnation point flow. The effect of the chemical reaction and magnetic field on the three-dimensional flow behavior of an elastic-viscous nanofluid over a stretching sheet was discovered by Ramzan and Bilal [6]. Sivasankaran et al. [7] investigated the effects of slip, chemical reaction,

*. *Corresponding author. Tel.: +91 7075223520*
E-mail addresses: gavi.lakshmidevi@vit.ac.in (G. Lakshmi Devi); hari.niranjan10@gmail.com (H. Niranjan); sivamaths@gmail.com (S. Sivasankaran)

doi: 10.24200/sci.2021.56835.4934

and radiation on mixed convection and convection boundary conditions of the viscous fluid flow on a plate. They found that with increasing the chemical reaction parameter, the rate of mass transfer increases while the rate of heat transfer falls.

The mass transfer process, as well as the chemical reaction and activation energy, has numerous applications in food processing, water mechanics, geothermal reservoirs, and oil emulsions, among others. Dhlamini et al. [8] investigated the effects of activation energy and chemical reaction in a mixed convective nanofluid flow with a convective boundary condition. They found that as the chemical reaction parameter increased, the thermophoresis increased. Makinde et al. [9] investigated the natural convection unsteady flow with nth order reaction under the influence of activation energy. Maleque [10] proposed an exothermic/endothermic reaction with activation energy in mixed convection flow. Hayat et al. [11] examined the characteristics of activation energy and exponential dependent heat source in Carreau fluid flow with cross-diffusion effect. Awad et al. [12] used the modified Arrhenius function to study the rotating flow of binary fluid over a deformed impulsive surface. Makinde and Gnaneswara Reddy [13] examined the effect of velocity slip on the peristaltic flow of electrically conducting Casson fluid in a channel embedded with a porous medium. They observed that when the magnetic field and Casson fluid parameters increased, the velocity and temperature profiles decreased. Anuradha and Yegammai [14] explored the combined effects of activation energy and radiation on the MHD chemically reacting nanofluid flow over a vertical plate. Nanofluid is a colloidal solution made up of nanoparticles ranging in size from 1 to 100 nm that are uniformly distributed in the whole base fluid. Nanofluids are used in a variety of industrial and engineering applications. The physical characteristics of Newtonian Carreau fluid immersed in the nanofluid near a point of stagnation towards thermal radiation stretching sheet were investigated by Zaib et al. [15]. Isa et al. [16] provided the explicit numerical analysis for a mixed convection MHD flow of Casson fluid over an infinitely permeable shrinking sheet. As the magnetic parameter, aligned angle, nanosolid volume fraction parameter, and slip parameter values increase, the temperature of the nano solid increases, as reported by Ganga et al. [17]. Ullah et al. [18] found that radiation and MHD flow have an impact on Marangoni convection nano liquids. They observed that the temperature increased when the radiation and heat generation/absorption parameters were increased. Nanofluids have the potential to provide substantial thermal enhancement with a lower pressure drop in comparison to water, according to Sivasankaran and Narrein[19]. Alsaadi et al. [20] explored the generation of entropy in the nonlinear convective mixed flow of nanofluid in porous space that is affected by thermal radiation and activation energy.

At very high temperatures, radiation affects the flow of heat and MHD, and understanding heat radiation transfer is crucial to the design of specific devices. In manufacturing industries, the heat radiative flow and mass transfer play an important role in the designing of aircraft, space vehicles, gas turbines, nuclear power plants, satellites, energy utilization, and numerous agricultural applications. Ganesh et al. [21] investigated the effect of radiation on incompressible hydromagnetic water-based nanofluid flow past a stretching sheet. Dar [22] and Kho et al. [23] analyzed numerically the effects of Casson nanofluid radiation on the heat of the MHD flow and mass transfer over a stretching sheet. Ullah et al. [24] observed the radiation parameter and nanoparticles volumetric fraction are qualitatively similar concerning temperature. In the presence of suction, Daniel et al. [25] explored the unsteady MHD flow of electrically conducting nanofluid past a stretching sheet with radiation and chemical reaction. Hamid et al. [26] and Chandrakala and Raj [27] studied the effect of radiation on MHD flow passing through an impulsively induced infinite vertical plate. Ahmed and Sarmah [28] examined the effect of magnetic field and thermal radiation on transient non-gray fluid flow past an impulsive vertical plate. Mukhopadhyay [29] studied the effects of thermal radiation on the mixed convection flow and transfer of heat over the porous stretching surface. Hayat et al. [30] discussed the Marangoni thermosolutal convective flow of nano liquid under the effect of space-dependent exponential thermal radiation and internal heat source.

Some natural and forced flows are affected, for example, by magnetic fields during pumping, stirring, and heating. Sheikholeslami et al. [31] studied the effect of radiative heat transfer on MHD non-Darcy nanofluid. The heat transfers on the MHD boundary layer flow over a stretching sheet were studied in [32-34]. They found that fluid velocity decreases when increasing the magnetic field parameter. Chutia and Deka [35] studied an unsteady and MHD Couette flow of incompressible, electrically conducting, viscous fluid between two infinitely long porous parallel plates in the presence of a transverse magnetic field. Devi et al. [36] examined the impact of heat and mass transfer on the MHD flow of an incompressible and radiating fluid over an exponentially stretched sheet, and they found that the fluid is thicker due to magnetic parameters. Under convective boundary surface conditions and over a vertical plate, Makinde and Olanrewaju [37] studied the effect of buoyancy forces on thermal boundary layers. Ramzan et al. [38] found that the velocity field would decrease to increase the value of the buoyancy ratio parameter. Under the effect of the chemical reaction and activation energy, Mustafa et al. [39]

conducted a numerical study on the convective flow of the magnetic nanofluid.

In light of all the above-mentioned works, we conducted a numerical study. The main purpose of this article is to explore the effects of thermal radiation, buoyancy, chemical reactions, and activation energy on the flow of two-dimensional MHD nanofluid flow past a stretching vertical surface. As far as we know, these combined effects on MHD buoyancy-induced nanofluidics have not occurred in the past. Using similarity transformation, the nonlinear governing equations are transformed into a system of ordinary differential equations. Using the Shooting technique, these transformed equations are then solved numerically. The graphs are used to explain the impact of physical parameters.

2. Mathematical formulation

Let us consider a steady, incompressible, laminar, MHD nanofluid flow over a vertical stretching sheet. In this problem, the combined effect of the chemical reaction and activation energy are considered. In the coordinate system (x, y), 'x' is chosen along the surface and 'y' is chosen normal to the surface. The velocity components u and v are taken as along x and y directions respectively (Figure 1).

B_0 is the intensity of the uniform magnetic field applied perpendicular to the stretchable sheet. Let us assume that the sheet surface is stretched by the linear velocity $u_w = ax$ in the vertical direction, where $a > 0$ indicates the stretching rate. Let us consider that at ambient state surface temperature T_w is greater than the fluid temperature. The governing equations could be written as:

$$\frac{\partial u}{\partial x} + \frac{\partial v}{\partial y} = 0, \tag{1}$$

$$u\frac{\partial u}{\partial x} + v\frac{\partial u}{\partial y} = \nu_f \frac{\partial^2 u}{\partial y^2} - \frac{\sigma^* B_0^2}{\rho_f} u + \frac{1}{\rho_f}\left[(1 - C_\infty)\rho_{f\infty}\beta(T - T_\infty) - (\rho_P - \rho_{f\infty})(C - C_\infty)\right] g, \tag{2}$$

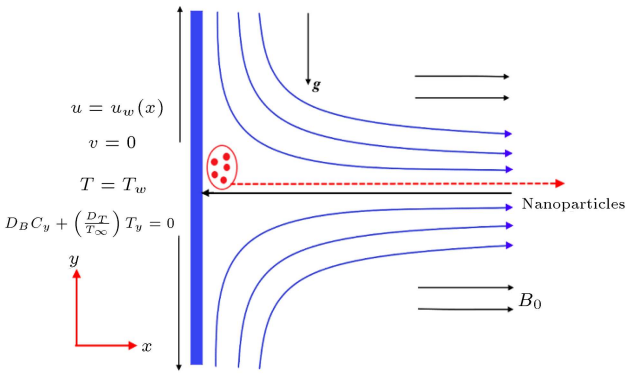

Figure 1. Schematic diagram of the problem.

$$u\frac{\partial T}{\partial x} + v\frac{\partial T}{\partial y} = \alpha\frac{\partial^2 T}{\partial y^2} + \tau\left[D_B\frac{\partial T}{\partial y}\frac{\partial C}{\partial y} + \frac{D_T}{T_\infty}\left(\frac{\partial T}{\partial y}\right)^2\right] - \frac{\alpha}{k}\frac{\partial q_r}{\partial y} + \beta K_r^2\left(\frac{T}{T_\infty}\right)^n \exp\left[\frac{-E_a}{KT}\right](S - S_\infty), \tag{3}$$

$$u\frac{\partial S}{\partial x} + v\frac{\partial S}{\partial y} = D\frac{\partial^2 S}{\partial y^2} - K_r^2(S - S_\infty)\left(\frac{T}{T_\infty}\right)^n \exp\left(\frac{-E_a}{KT}\right), \tag{4}$$

$$u\frac{\partial C}{\partial x} + v\frac{\partial C}{\partial y} = D_B\frac{\partial^2 C}{\partial y^2} + \frac{D_T}{T_\infty}\frac{\partial^2 T}{\partial y^2}, \tag{5}$$

where $\alpha = \frac{k}{(\rho c)_f}$ and $\tau = \frac{(\rho c)_p}{(\rho c)_f}$. Subject to the boundary conditions for the present problem is as follows:

$$u = u_w(x) = cx, \quad v = 0, \quad D_\infty\frac{\partial C}{\partial y} + \frac{D_T}{T_\infty}\frac{\partial T}{\partial y} = 0,$$

$$-k\frac{\partial T}{\partial y} = h_f(T_f - T), \quad S = S_w \quad \text{at} \quad y = 0$$

$$u \to 0,\ T \to T_\infty,\ C \to C_\infty,\ S \to S_\infty \quad \text{at} \quad y \to \infty, \tag{6}$$

where u and v are the velocity components in the (x, y) axes, respectively. The temperature of the fluid is T, the kinematic viscosity of a fluid is $\nu = \frac{\mu}{\rho}$ and the thermal conductivity is k. The radiative heat flux q_r is given by:

$$q_r = -\frac{4\sigma^*}{3K'}\frac{\partial T^4}{\partial y}. \tag{7}$$

The heat flux (q_r) radiative term in Eq. (3) is simplified using the Rosseland approximation. Using Taylor series we can extend T^4 about T_∞ and ignore higher-order terms. It can be expressed as a linear function of temperature T, i.e., $T^4 = T_\infty^4 + 4T_\infty^3(T - T_\infty) + \cdots$ then:

$$T^4 \approx 4T_\infty^3 T - 3T_\infty^4.$$

Finally, we get:

$$q_r = -\frac{16\sigma^* T_\infty^3}{3K'}\frac{\partial T}{\partial y}. \tag{8}$$

Now we define the following non-dimensional functions $f(\eta)$, $\theta(\eta)$, $\chi(\eta)$, $\phi(\eta)$ and similarity variable η as:

$$\eta = \sqrt{\frac{c}{\nu}}y, \qquad \psi(x, y) = \sqrt{c\nu}\, x f(\eta),$$

$$v = -\sqrt{c\nu} f(\eta), \qquad \theta(\eta) = \frac{T - T_\infty}{T_w - T_\infty},$$

$$\chi(\eta) = \frac{S - S_\infty}{S_w - S_\infty}, \qquad \phi(\eta) = \frac{C - C_\infty}{C_W - C_\infty}. \tag{9}$$

The stream function $\psi(x, y)$ is defined as:

$$u = \frac{\partial \psi}{\partial y} \qquad \text{and} \qquad v = -\frac{\partial \psi}{\partial x}. \tag{10}$$

The governing equations (Eqs. (1)–(5)) are transformed into the ordinary differential equations by using Eqs. (8)–(10) as follows:

$$f''' - f'^2 + f f'' - M f' + \lambda(\theta - Nr\phi) = 0, \tag{11}$$

$$\theta''\left(1 + \frac{4}{3}Rd\right) + \Pr f\theta' + Nb\Pr\theta'\phi' + Nt\Pr\theta'^2 + \Pr\sigma Nc[1 + \theta\delta]^n \exp\left(\frac{-E}{1 + \theta\delta}\right) = 0, \tag{12}$$

$$\chi'' + Scf\chi' - Sc\sigma\chi(1 + \theta\delta)^n \exp\left(\frac{-E}{1 + \theta\delta}\right) = 0, \tag{13}$$

$$\phi'' + Scf\phi' + \left(\frac{Nt}{Nb}\right)\theta'' = 0. \tag{14}$$

The corresponding boundary conditions, Eq. (6), is as follows:

$$f'(0) = 1, \quad f(0) = 0, \quad \phi'(0) = -\left(\frac{Nt}{Nb}\right) * \theta'(0),$$

$$\theta'(0) = -Bi[1 - \theta(0)], \quad \chi(0) = 1 \quad \text{at} \quad \eta \to 0$$

$$f'(\infty) = 0, \quad \theta(\infty) = 0, \quad \phi(\infty) = 0, \quad \chi(\infty) = 0$$

$$\text{as} \quad \eta \to \infty. \tag{15}$$

Now we introduce the following dimensionless quantities:

$$\lambda = \frac{g\beta(1 - C_\infty)(T_w - T_\infty)}{C^2 x} = \frac{Gr_x}{Re_x^2},$$

$$Gr_x = \frac{g\beta(1 - C_\infty)(T_w - T_\infty)x^3}{\nu^2}, \quad Re_x = \frac{u_w x}{\nu}$$

$$M = \frac{\sigma^* B_0^2}{\rho_f c}, \quad Nr = \frac{(\rho_p - \rho_{f\infty})C_\infty}{\rho_{f\infty}\beta(1 - C_\infty)(T_w - T_\infty)},$$

$$Pr = \frac{\nu_f}{\alpha_f}, \quad Nb = \frac{\tau D_B C_\infty}{\nu_f},$$

$$Nt = \frac{\tau D_T(T_w - T_\infty)}{T_\infty \nu_f}, \quad Sc = \frac{\nu_f}{D_B}, \quad \sigma = \frac{k_r^2}{c},$$

$$E = \frac{E_a}{KT_\infty}, \quad \delta = \frac{T_w - T_\infty}{T_\infty}, \quad Nc = \frac{\beta(S - S_\infty)}{T_w - T_\infty},$$

$$Rd = \frac{4\sigma^* T_3^\infty}{kK'}. \tag{16}$$

The physical quantities describing the skin friction (C_f), the Local Nusselt number (Nu_x), the local Sherwood number (Sh_x), and the local nanoparticle Sherwood number (Nn_x) are shown below:

$$C_f = \frac{\tau_w}{\rho U_w^2}, \qquad Nu_x = \frac{xq_w}{k(T - T_\infty)},$$

$$Sh_x = \frac{xq_s}{D_s(S - S_\infty)}, \quad Nn_x = \frac{xq_n}{D_B(C - C_\infty)},$$

$$\text{where} \quad \tau_w = \left[\frac{\partial u}{\partial y}\right]_{y=0}, \quad q_w = -k\left[\frac{\partial T}{\partial y}\right]_{y=0},$$

$$q_s = -D_s\left[\frac{\partial S}{\partial y}\right]_{y=0}, \quad q_n = -D_B\left[\frac{\partial C}{\partial y}\right]_{y=0}. \tag{17}$$

Using the non-dimensional functions and similarity variable given in Eq. (9), we obtain:

$$C_f(Re_x)^{\frac{1}{2}} = f''(0), \quad \frac{Nu_x}{(Re_x)^{\frac{1}{2}}} = -\theta'(0),$$

$$\frac{Sh_x}{(Re_x)^{\frac{1}{2}}} = -\chi'(0), \quad \frac{Nn_x}{(Re_x)^{\frac{1}{2}}} = -\phi'(0), \tag{18}$$

where $Re_x = \frac{xU_w(x)}{\nu}$ is defined as the local Reynold number.

3. Results and discussion

This study considered the combined effects of chemical reactions, activation energy, thermal radiation, and buoyancy on the flow of the MHD nanofluids flow on a stretching vertical surface. By using appropriate boundary conditions, the governing problem is solved numerically by the MATLAB bvp4c. The present numerical results are compared with the results of Mustafa et al. [39] for dissimilar values, and they are exposed in Table 1. This provides certainty for the numerical results we will communicate later. The effect of local Nusselt number $-\theta'(0)$, thermophoresis parameter (Nt) and mixed convection parameter (λ) are tabulated. It can be seen that as the local Nusselt number increases, the Prandtl number and mixed convection parameters increase, and the thermophoresis parameter decreases.

Figures 2 and 3 depict the effect of various values of regular buoyancy parameters (Nc) on the velocity profile ($f'(\eta)$) and solute concentration profile ($\chi(\eta)$). Figure 2 shows the increment of the velocity of the fluid with regular buoyancy parameter and gradual decrement in the thickness of the boundary layer. As is clear from Figure 3, the value (Nc) increases as the value of the solute concentration profile decreases, and the thickness of the boundary layer gradually decreases.

Table 1. Comparison of wall slope of temperature $-\theta'(0)$ values with findings of Mustafa et al. [39] for $M = Nr = 0.5$, $\delta = 1$, and $Sc = 5$.

Pr	Nt	E	σ	n	λ	Mustafa et al. [39]	Present study
2	0.5	1	1	0.5	0.5	0.706605	0.706831
4	–	–	–	–	–	0.935952	0.936056
7	–	–	–	–	–	1.132787	1.132900
10	–	–	–	–	–	1.257476	1.257032
5	0.1	1	1	0.5	0.5	1.426267	1.426012
–	0.5	–	–	–	–	1.013939	1.038594
–	0.7	–	–	–	–	0.846943	0.846593
–	1.0	–	–	–	–	0.649940	0.649752
10	0.5	1	2	0.5	0.0	1.032281	1.032085
0.5	–	–	–	–	–	1.056704	1.056294
3.0	–	–	–	–	–	1.154539	1.154956
5.0	–	–	–	–	–	1.215937	1.216012

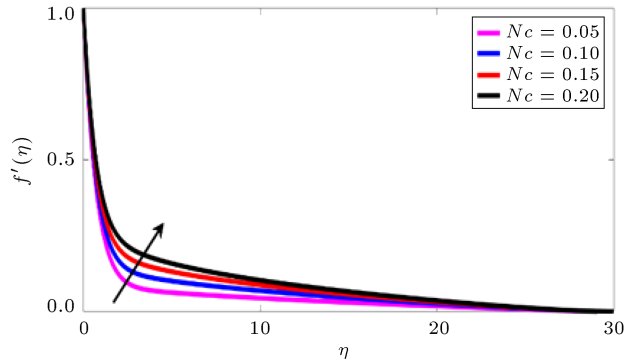

Figure 2. Velocity profile for various values of regular buoyancy parameter Nc, when $M = 0.1$, $\lambda = -1, Pr = 7, Rd = 0.3, E = 2$, $Nb = Nr = Nt = n = 0.5, \delta = \sigma = Bi = Sc = 1$.

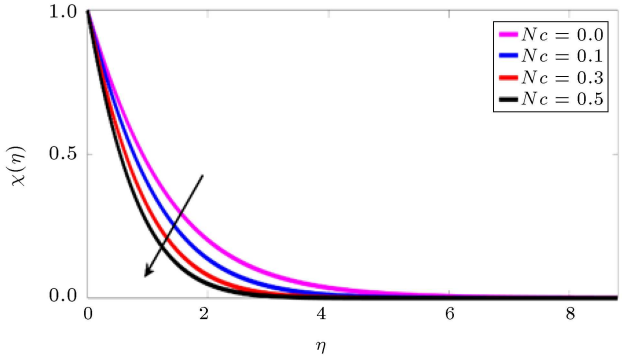

Figure 3. Solute concentration profile for various values of regular buoyancy parameter Nc, when $Nr = 0.1$, $Pr = 7$, $Rd = 0.3$, $E = 2$, $\lambda = Nb = Nt = n = 0.5$, $\delta = \sigma = M = Bi = Sc = 1$.

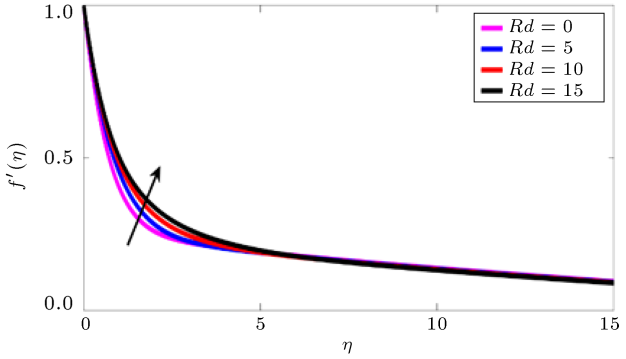

Figure 4. Velocity profile for various values of thermal radiation parameter Rd, when $Nc = 0.1$, $Pr = 7$, $E = Nb = Nr = Nt = 0.5, \delta = \lambda = \sigma = M = Bi = Sc = n = 1$.

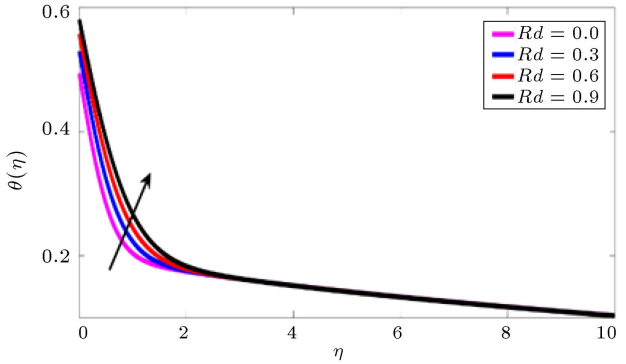

Figure 5. Temperature profile for various values of thermal radiation parameter Rd, when $Nc = 0.2$, $Pr = 7, \sigma = Nr = 0.1, \lambda = Nb = Nt = n = 0.5, \delta = E = M = Bi = Sc = 1$.

Figure 4 to Figure 6 indicate the effect of diverse values of thermal radiation (Rd) on velocity profile ($f'(\eta)$), temperature profile ($\theta(\eta)$), and nanoparticle concentration profile respectively. Here, as the thermal radiation parameters increase, the velocity, temperature, and liquid concentration increase, creating a thin boundary layer that gradually decreases. Through thermal radiation, we can control the fluid temperature because the temperature is very sensitive to thermal radiation. This means more heat flux at the surface. Figure 7 shows the impact of Biot number (Bi) on the

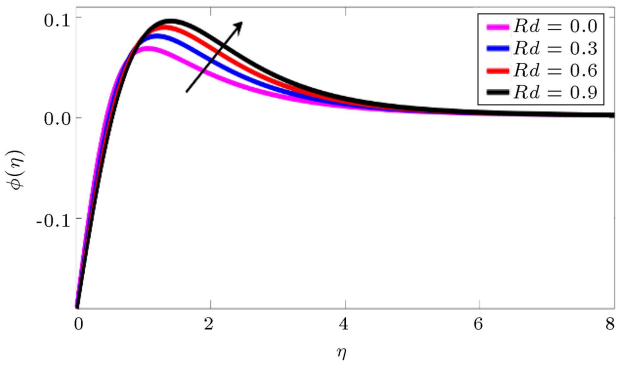

Figure 6. Nanoparticle concentration profile for various values of thermal radiation parameter Rd, when $Nc = 0.2, Pr = 7, \sigma = Nr = 0.1, \lambda = Nb = Nt = n = 0.5, \delta = E = M = Bi = Sc = 1$.

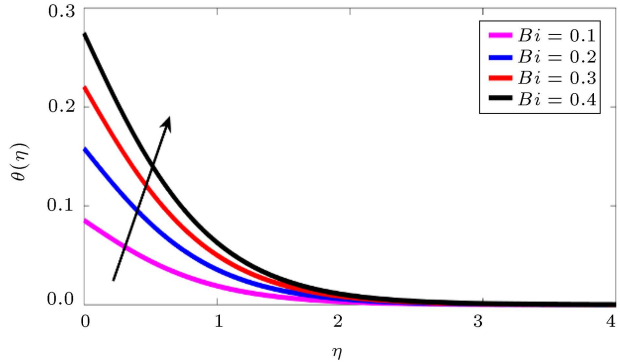

Figure 7. Temperature profile for various values of Biot number Bi, when $Nc = 0.2, Rd = 0.3, Pr = 7, \sigma = Nr = 0.1, \delta = E = M = Sc = 1, \lambda = Nb = Nt = n = 0.5$.

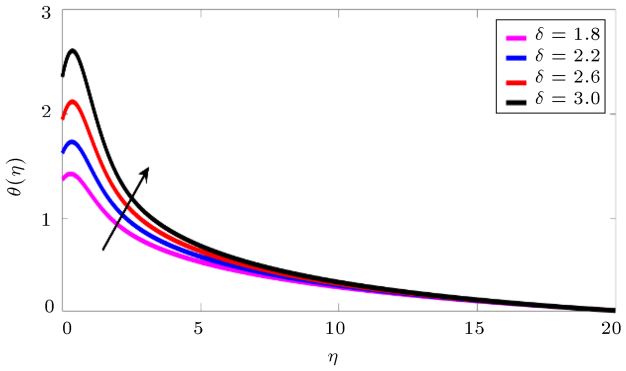

Figure 8. Temperature profile for various values of temperature difference parameter δ, when $Pr = 5, Nc = Nr = Rd = 0.1, \lambda = Nb = Nt = 0.5, \sigma = E = M = Bi = Sc = n = 1$.

temperature profile. It shows that the temperature of the fluid increases and the boundary layer decreases gradually as the values of (Bi) increase. The increase in Biot number is associated with low Brownian motion, which helps to spread the concentration quickly on the surface. Figures 8 and 9 show the effect of different values of temperature difference parameters (δ)

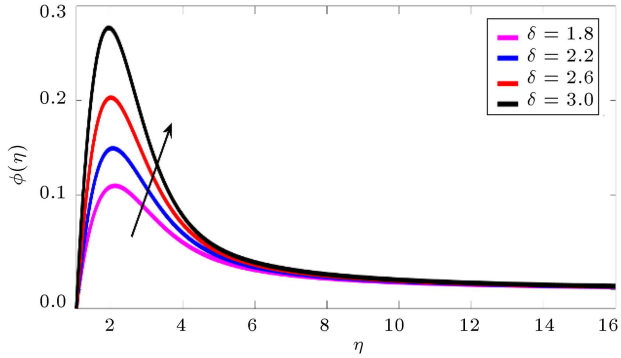

Figure 9. Nanoparticle concentration profile for various values of temperature difference parameter δ, when $Pr = 5, Nc = Nr = Rd = 0.1, Nb = Nt = \lambda = 0.5, \sigma = E = M = Bi = Sc = n = 1$.

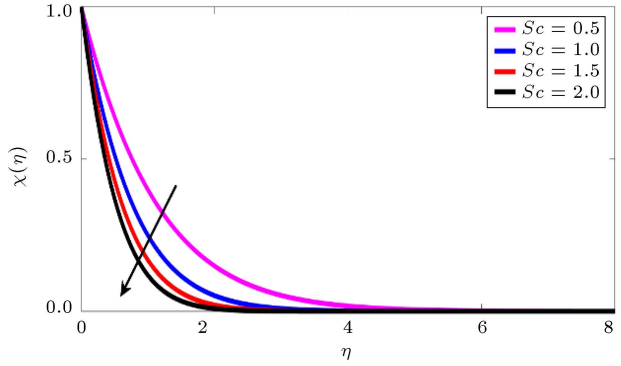

Figure 10. Solute concentration profile for various values of Schmidt number Sc, when $Pr = 5, Nr = Nc = Rd = 0.1, \lambda = Nb = Nt = 0.5, \delta = \sigma = E = M = Bi = n = 1$.

on temperature profile and nanoparticle concentration profile respectively. Figures 8 and 9 illustrate that the temperature and nanoparticle concentration profile increase as the values of 'δ' increase, and the thickness of the boundary layer decreases gradually. The impact of various values of the Schmidt number (Sc) on the solute concentration profile is shown in Figure 10. It is observed that the Schmidt number increases as the concentration of solute decreases and the thickness of the corresponding boundary layer decrease rapidly. Figure 11 shows the effect of various values of non-dimensional activation energy (E) on the velocity profile. It can be seen that the fluid velocity decreases as 'E' increases, and the thickness of the boundary layer gradually decreases.

Figure 12 shows the increase of skin friction by increasing the values of regular buoyancy parameter (Nc) and fitted rate constant 'n', i.e., friction on the vertical surface is increased. Figure 13 illustrates the local Nusselt number for varying values of regular buoyancy parameter 'Nc', against the fitted rate constant. From the stretching boundary, it is clear that heat flux is inversely proportional to the regular buoyancy force. Moreover, $-\theta'(0)$ decays in a

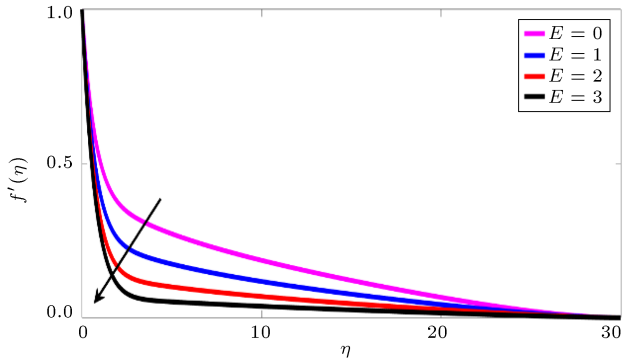

Figure 11. Velocity profile for various values of non-dimensional activation energy E, when $Pr = 7, Nc = 0.1, Rd = 0.3, \lambda = Nb = Nr = Nt = n = 0.5, \delta = \sigma = M = Bi = Sc = 1$.

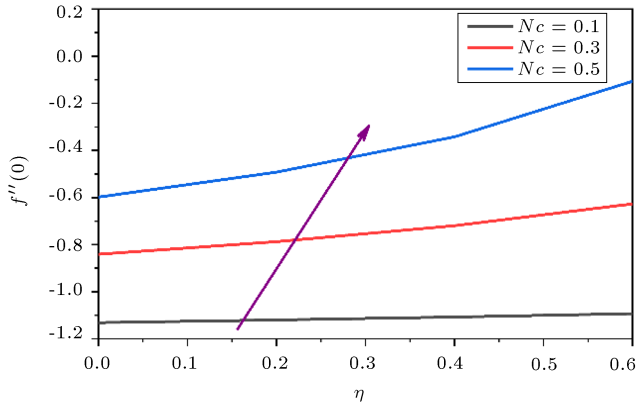

Figure 12. Skin friction for various values of Nc and n, when $Pr = 7, Nr = 0.1, Rd = 0.3, Nb = Nt = \lambda = 0.5, \delta = \sigma = E = M = Bi = Sc = 1$.

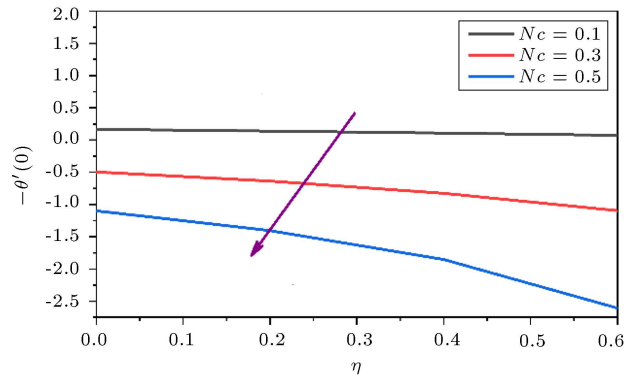

Figure 13. Local Nusselt number for various values of Nc and n, when $Pr = 7, Nr = 0.1, Rd = 0.3, \lambda = Nb = Nt = 0.5, \delta = \sigma = E = M = Bi = Sc = 1$.

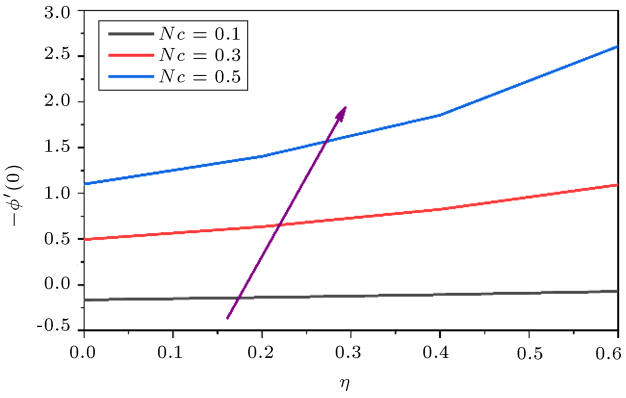

Figure 14. Local nanoparticle Sherwood number for various values of Nc and n, when $Pr = 7, Nr = 0.1, Rd = 0.3, \lambda = Nb = Nt = 0.5, \delta = \sigma = E = M = Bi = Sc = 1$.

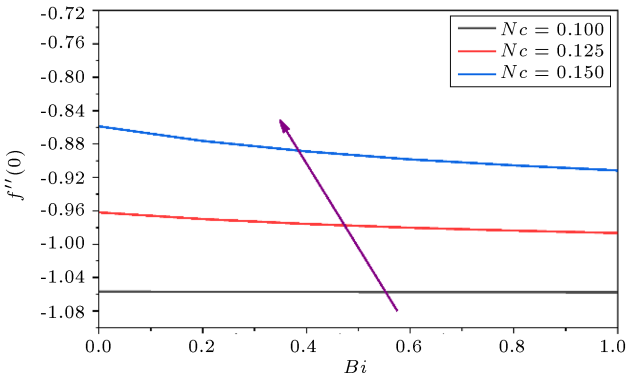

Figure 15. Skin friction for various values of Nc and Bi, when $Pr = 5, Nr = 0.1, Rd = 0.3, \lambda = Nb = Nt = 0.5, \delta = \sigma = E = M = Sc = n = 1$.

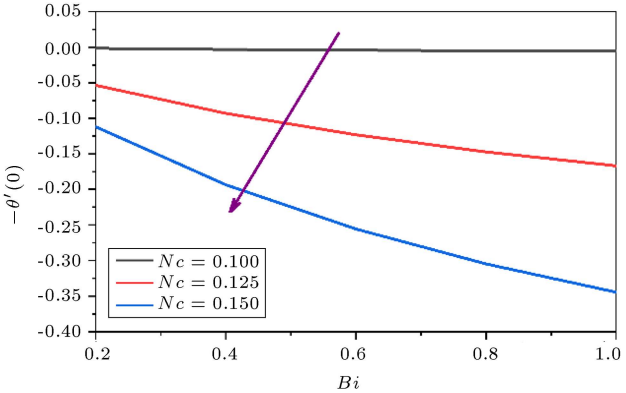

Figure 16. Local Nusselt number for various values of Nc and Bi, when $Pr = 5, Nr = 0.1, Rd = 0.3, \lambda = Nb = Nt = 0.5, \delta = \sigma = E = M = Sc = n = 1$.

nonlinear fashion when 'n' increases. For the increment of regular buoyancy parameter (Nc) and fitted rate constant the local nanoparticle Sherwood numbers and the layer thickness increases as shown in Figure 14. It indicates the effectiveness of mass convection on the surface. Figure 15 depicts skin friction with regular buoyancy parameters and Biot number. It is observed that the vertical surface friction increases with 'Nc', but decreases with 'Bi' and layer thickness decreases gradually. Figure 16 depicts the reduced heat transfer rate with increased regular buoyancy parameter and increased thermal flux with Biot number.

The local Sherwood number decreases as the Biot number increases, as shown in Figure 17. The heat

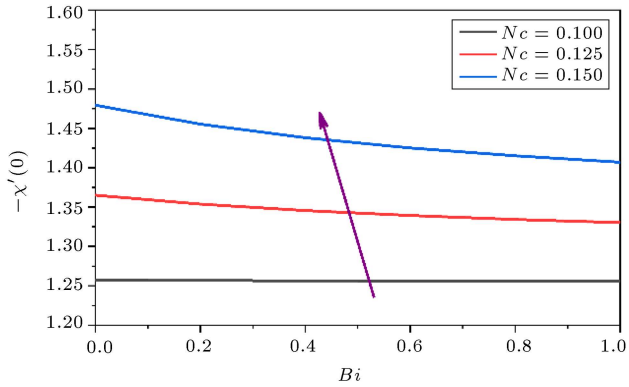

Figure 17. Local Sherwood number for various values of NC and Bi, when $Pr = 5, Nr = 0.1, Rd = 0.3, \lambda = Nb = Nt = 0.5, \delta = \sigma = E = M = Sc = n = 1$.

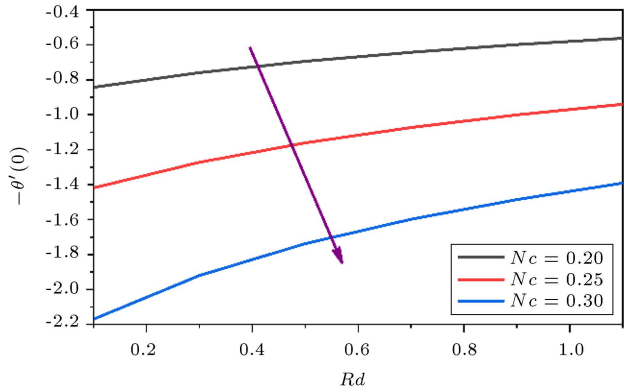

Figure 18. Local Nusselt number for various values of Nc and Rd, when $Pr = 5, \sigma = Nr = 0.1, \lambda = Nb = Nt = 0.5, \delta = E = M = Bi = Sc = n = 1$.

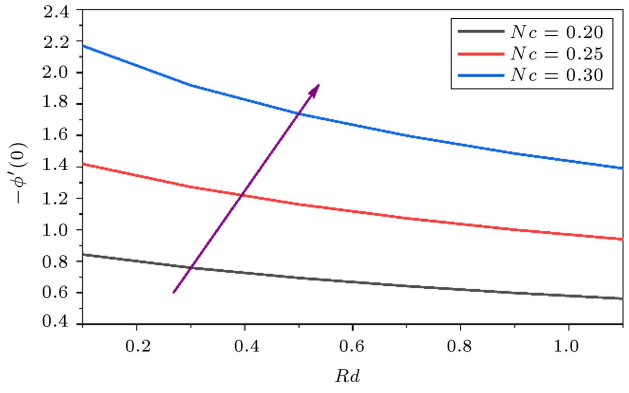

Figure 19. Local nanoparticle Sherwood number for various values of Nc and Rd, when $Pr = 5, \sigma = Nr = 0.1, \lambda = Nb = Nt = 0.5, \delta = E = M = Bi = Sc = n = 1$.

transfer flow decreases as the regular buoyancy parameter increases, but as the thermal radiation increases, the layer thickness decreases, as shown in Figure 18. Figure 19 clearly shows the increase in Sherwood's number of local nanoparticles with regular buoyancy parameters. But as the thermal radiation increases, the Sherwood number of local nanoparticles decreases.

4. Conclusion

The collective impact of chemical reaction, activation energy, thermal radiation, and buoyancy force on magnetohydrodynamic (MHD) nanofluid flow over a stretching vertical surface is described numerically. Our investigation revealed the following:

- The velocity profile over the vertical surface increases with the increase of regular buoyancy parameters and thermal radiation but decreases with the increase of activation energy;
- The temperature of the fluid raises with the increase of thermal radiation, Biot number, and temperature difference parameter;
- Nanoparticle concentration of the fluid is increases on increasing the thermal radiation and temperature difference parameter;
- The fluid solute concentration reduces on increasing of regular buoyancy parameter and Schmidt number;
- Skin friction of the fluid at the vertical surface increases with regular buoyancy parameter and fitted rate constant, i.e. velocity of the fluid is decreasing. But Skin friction reduces with increasing the Biot number and thermal radiation, i.e. fluid velocity is increasing.

Nomenclature

B_0	Strength of magnetic field
C	Concentration
D_B	Brownian diffusion coefficient
D_T	Thermophoretic diffusion coefficient
E	Nondimensional activation energy
E_a	Activation energy
F'	Dimensionless velocity
Gr_x	Local Grashof number
g	Gravitational acceleration
K	Boltzmann constant
K'	Mean absorption coefficient
k	Thermal conductivity
k_r^2	Reaction rate
M	Magnetic field parameter
Nb	Brownian diffusion parameter
Nc	Regular buoyancy parameter
Nr	Buoyancy ratio parameter
Nt	Thermophoresis parameter
n	Fitted rate constant
Pr	Prandtl number of base fluid
q_r	Radiative heat flux

Rd	Thermal radiation parameter
Re_x	Local Reynolds number
Sc	Schmidt number
T	Temperature

Greek symbols

λ	Mixed convection parameter
σ	Dimensionless reaction rate
δ	Temperature difference parameter
v	Kinematic viscosity
σ_e	Electrical conductivity
σ^*	Stefan-Boltzmann constant
ρ_f	Density of the fluid
β	Coefficient of thermal expansion
ρ_p	Nanoparticle density
α	Thermal diffusivity of the base fluid
τ	Ratio of the effective heat capacity of the nanoparticle material and the heat capacity of the fluid
$(\rho c)_f$	Heat capacity of the base fluid
$(\rho c)_p$	Effective heat capacity of the nanoparticle material
θ	Dimensionless temperature
χ	Dimensionless solute concentration
ϕ	Dimensionless nanoparticle concentration

Subscripts

w	Condition on the wall
∞	Condition at free stream

References

1. Ibrahim, S.Y. and Makinde, O.D. "Chemically reacting magnetohydrodynamics (MHD) boundary layer flow of heat and mass transfer past a low-heat-resistant sheet moving vertically downwards", *Sci. Res. Essays*, **6**(22), pp. 4762–4775 (2011).
2. Jabeen, S., Hayat, T., Alsaedi, A., and Alhodaly, M.Sh. "Consequences of activation energy and chemical reaction in radiative flow of tangent hyperbolic nanoliquid", *Sci. Iran.*, **26**(6), pp. 3928–3937 (2019).
3. Niranjan, H., Sivasankaran, S., and Bhuvaneswari, M. "Chemical reaction, Soret and Dufour effects on MHD mixed convection stagnation point flow with radiation and slip condition", *Sci. Iran.* , **24**(2), pp. 698–706 (2017).
4. Mallikarjuna, B., Rashad, A.M., Chamkha, A.J., and Raju, S.H. "Chemical reaction effects on MHD convective heat and mass transfer flow past a rotating vertical cone embedded in a variable porosity regime", *Afr. Mat.*, **27**(3), pp. 645–665 (2016).
5. Hayat, T., Ullah, I., Alsaedi, A., and Asghar, S. "Flow of magneto Williamson nanoliquid towards stretching sheet with variable thickness and double stratification", *Radiat. Phys. Chem.*, **152**, pp. 151–157 (2018).
6. Ramzan, M. and Bilal, M. "Three-dimensional flow of an elastico-viscous nanofluid with chemical reaction and magnetic field effects", *J. Mol. Liq.*, **215**, pp. 212–220 (2016).
7. Sivasankaran, S., Niranjan, H., and Bhuvaneswari, M. "Chemical reaction, radiation and slip effects on MHD mixed convection stagnation-point flow in a porous medium with convective boundary condition", *Int. J. Numer. Methods Heat Fluid Flow*, **27**(2), pp. 454–470 (2017).
8. Dhlamini, M., Kameswaran, P.K., Sibanda, P., Motsa, S., and Mondal, H. "Activation energy and binary chemical reaction effects in mixed convective nanofluid flow with convective boundary conditions", *J Comput Des Eng*, **6**(2), pp. 149–158 (2019).
9. Makinde, O.D., Olanrewaju, P.O., and Charles, W.M. "Unsteady convection with chemical reaction and radiative heat transfer past a flat porous plate moving through a binary mixture", *Afr. Mat.*, **22**(1), pp. 65–78 (2011).
10. Maleque, K.A. "Effects of exothermic/endothermic chemical reactions with Arrhenius activation energy on MHD free convection and mass transfer flow in presence of thermal radiation", *J. Thermodyn.*, **2013**, pp. 1–11 (2013).
11. Hayat, T., Ullah, I., Waqas, M., and Alsaedi, A. "Attributes of activation energy and exponential based heat source in flow of Carreau fluid with cross-diffusion effects", *J Non-Equil Thermody*, **44**(2), pp. 203–213 (2019).
12. Awad, F.G., Motsa, S., and Khumalo, M. "Heat and mass transfer in unsteady rotating fluid flow with binary chemical reaction and activation energy", *PLoS One*, **9**(9), e107622 (2014).
13. Makinde, O.D. and Gnaneswara Reddy, M. "MHD peristaltic slip flow of Casson fluid and heat transfer in channel filled with a porous medium", *Sci. Iran.*, **26**(4), pp. 2342–2355 (2019).
14. Anuradha, S. and Yegammai, M. "MHD radiative boundary layer flow of nanofluid past a vertical plate with effects of binary chemical reaction and activation energy", *Glob J. Pure Appl. Math.*, **13**(9), pp. 6377–6392 (2017).
15. Zaib, A., Rashidi, M.M., Chamkha, A.J., and Mohammad, N.F. "Impact of nonlinear thermal radiation on stagnation-point flow of a Carreau nanofluid past a nonlinear stretching sheet with binary chemical reaction and activation energy", *Proc Inst Mech Eng C:J Mech Eng Sci.*, **232**(6), pp. 962–972 (2018).

16. Isa, S.S.P.M., Arifin, N.M., Nazar, R., Bachok, N., Ali, F.M., and Pop, I. "MHD mixed convection boundary layer flow of a Casson fluid bounded by permeable shrinking sheet with exponential variation", *Sci. Iran.*, **24**(2), pp. 637–647 (2017).

17. Ganga, B., Govindaraju, M., and Hakeem, A.A. "Effects of inclined magnetic field on entropy generation in nanofluid over a stretching sheet with partial slip and nonlinear thermal radiation", *Iran J. Sci. Technol.-Trans. Mech. Eng.*, **43**(4), pp. 707–718 (2019).

18. Ullah, I., Hayat, T., Alsaedi, A., and Asghar, S. "Modeling for radiated Marangoni convection flow of magneto-nanoliquid subject to Activation energy and chemical reaction", *Sci. Iran.*, **27**(6), pp. 3390–3398 (2020).

19. Sivasankaran, S. and Narrein, K. "Influence of geometry and magnetic field on convective flow of nanofluids in trapezoidal microchannel heat sink", *Iran J. Sci. Technol.-Trans. Mech. Eng*, **44**(22), pp. 373–382 (2020).

20. Alsaadi, F.E., Ullah, I., Hayat, T., and Alsaadi, F.E. "Entropy generation in nonlinear mixed convective flow of nanofluid in porous space influenced by Arrhenius activation energy and thermal radiation", *J. Therm. Anal. Calorim.*, **140**, pp. 799–809 (2020).

21. Ganesh, N.V., Hakeem, A.K., Jayaprakash, R., and Ganga, B. "Analytical and numerical studies on hydromagnetic flow of water based metal nanofluids over a stretching sheet with thermal radiation effect", *J. Nanofluids*, **3**(2), pp. 154–161 (2014).

22. Dar, A.A. "Effect of thermal radiation, temperature jump and inclined magnetic field on the peristaltic transport of blood flow in an asymmetric channel with variable viscosity and heat absorption/generation", *Iran J. Sci. Technol.-Trans. Mech. Eng.*, **45**(2), pp. 487-501 (2021).

23. Kho, Y.B., Hussanan, A., Sarif, N.M., Ismail, Z., and Salleh, M.Z. "Thermal radiation effects on MHD with flow heat and mass transfer in Casson nanofluid over a stretching sheet", *MATEC Web Conf. EDP Sciences*, **150**, pp. 1–6 (2018).

24. Ullah, I., Hayat, T., Alsaedi, A., and Asghar, S. "Dissipative flow of hybrid nanoliquid (H_2O-aluminum alloy nanoparticles) with thermal radiation", *Phys. Scr.*, **94**(12), pp. 1–15 (2019).

25. Daniel, Y.S., Aziz, Z.A., Ismail, Z., and Salah, F. "Thermal radiation on unsteady electrical MHD flow of nanofluid over stretching sheet with chemical reaction", *J. King Saud Univ. Sci.*, **31**(4), pp. 804–812 (2019).

26. Hamid, M., Usman, M., Khan, Z.H., Haq, R.U., and Wang, W. "Numerical study of unsteady MHD flow of Williamson nanofluid in a permeable channel with heat source/sink and thermal radiation", *Eur. Phys. J. Plus*, **133**(12), pp. 1–12 (2018).

27. Chandrakala, P. and Raj, S.A. "Radiation effects on MHD flow past an impulsively started infinite isothermal vertical plate", *Indian J Chem Tech.*, **5**, pp. 63–67 (2008).

28. Ahmed, N. and Sarmah, H.K. "Thermal radiation effect on a transient MHD flow with mass transfer past an impulsively fixed infinite vertical plate", *Int. J. Appl. Math. Mech.*, **5**, pp. 87–98 (2009).

29. Mukhopadhyay, S. "Effect of thermal radiation on unsteady mixed convection flow and heat transfer over a porous stretching surface in porous medium", *Int. J. Heat Mass Transf.*, **52**(13–14), pp. 3261–3265 (2009).

30. Hayat, T., Ullah, I., Waqas, M., and Alsaedi, A. "Simulation of nanofluid thermal radiation in Marangoni convection flow of non-Newtonian fluid", *Int. J. Numer. Methods Heat Fluid Flow*, **29**(8), pp. 2840–2853 (2019).

31. Sheikholeslami, M., Li, Z., and Shamlooei, M.J.P.L.A. "Nanofluid MHD natural convection through a porous complex shaped cavity considering thermal radiation", *Phys. Lett. A.*, **382**(24), pp. 1615–1632 (2018).

32. Ishak, A. "MHD boundary layer flow due to an exponentially stretching sheet with radiation effect", *Sains Malays.*, **40**(4), pp. 391–395 (2011).

33. Jhankal, A.K. and Kumar, M. "MHD boundary layer flow past a stretching plate with heat transfer", *Int. J. Eng. Sci.*, **2**(3), pp. 9–13 (2013).

34. Seini, Y.I. and Makinde, O.D. "MHD boundary layer flow due to exponential stretching surface with radiation and chemical reaction", *Math. Probl. Eng.*, **2013**, pp. 1–7 (2013).

35. Chutia, M. and Deka, P.N. "Numerical solution of unsteady MHD couette flow in the presence of uniform suction and injection with hall effects", *Iran J. Sci. Technol.- Trans. Mech. Eng.*, **45**(2), pp. 503-514 (2021).

36. Devi, R.R., Poornima, T., Reddy, N.B., and Venkataramana, S. "Radiation and mass transfer effects on MHD boundary layer flow due to an exponentially stretching sheet with heat source", *Int J Eng Innov Tech.*, **3**(8), pp. 33–39 (2014).

37. Makinde, O.D. and Olanrewaju, P.O. "Buoyancy effects on thermal boundary layer over a vertical plate with a convective surface boundary condition", *J. Fluids Eng.*, **132**(4), pp. 1–4 (2010).

38. Ramzan, M., Ullah, N., Chung, J.D., Lu, D., and Farooq, U. "Buoyancy effects on the radiative magneto Micropolar nanofluid flow with double stratification, activation energy and binary chemical reaction", *Sci. Rep.*, **7**(1), pp. 1–15 (2017).

39. Mustafa, M., Khan, J.A., Hayat, T., and Alsaedi, A. "Buoyancy effects on the MHD nanofluid flow past a vertical surface with chemical reaction and activation energy", *Int J Heat Mass Transf.*, **108**, pp. 1340–1346 (2017).

Biographies

Gavireddy Lakshmi Devi is pursuing her PhD program at Vellore Institute of Technology, Vellore, Tamilnadu, India. She completed her MSc in the year 2019 at Yogi Vemana University, Kadapa, Andhra Pradesh, India. Her research interests are Fluid Dynamics, Numerical Heat Transfer, Boundary-Layer theory.

Hari Niranjan obtained MSc in Applied Mathematics from the National Institute of Technology, Warangal, India, and PhD in Mathematics from the University of Malaya, Kuala Lumpur, Malaysia. He has 16 years of teaching and research experience in India and abroad. He was a Senior Lecturer at Asia Pacific University, Kuala Lumpur, Malaysia. Presently, he is a Senior Assistant Professor of Mathematics at Vellore Institute of Technology, Vellore, Tamilnadu, India. His research interests are nanofluids, numerical methods boundary layer theory and numerical heat transfer.

Sivanandam Sivasankaran received his MSc, MPhil and PhD degrees from Bharathiar University, India. He received Post-Doctoral Fellowship at National Cheng Kung University, Taiwan and National Taiwan University, Taiwan. He was a Research Professor at Yonsei University, South Korea. Presently, He is an Associate Professor of Mathematics, King Abdulaziz University, Jeddah, Saudi Arabia. He is a member of the editorial board in several international journals and reviewers of more than 30 international journals. His areas of interest are convective heat and mass transfer, CFD, nanofluids, micro-channel heat sinks, and porous media.